

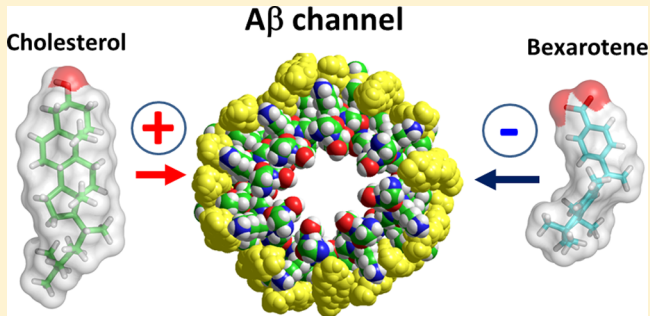
Bexarotene Blocks Calcium-Permeable Ion Channels Formed by Neurotoxic Alzheimer's β -Amyloid Peptides

Jacques Fantini,* Coralie Di Scala, Nouara Yahi, Jean-Denis Troadec, Kevin Sadelli, Henri Chahinian, and Nicolas Garmy

Aix-Marseille Université, EA4674, Faculté des Sciences de Saint-Jérôme, 13013 Marseille, France

ABSTRACT: The anticancer drug bexarotene has been shown to restore cognitive functions in animal models of Alzheimer's disease, but its exact mechanism of action remains elusive. In the present report, we have used a combination of molecular, physicochemical, and cellular approaches to elucidate the mechanisms underlying the anti-Alzheimer properties of bexarotene in neural cells. First of all, we noticed that bexarotene shares a structural analogy with cholesterol. We showed that cholesterol and bexarotene compete for the same binding site in the C-terminal region of Alzheimer's β -amyloid peptide 1–42 ($A\beta_{1-42}$). This common bexarotene/cholesterol binding domain was characterized as a linear motif encompassing amino acid residues 25–35 of $A\beta_{1-42}$. Because cholesterol is involved in the oligomerization of Alzheimer's β -amyloid peptides into neurotoxic amyloid channels, we studied the capability of bexarotene to interfere with this process. We showed that nanomolar concentrations of bexarotene efficiently prevented the cholesterol-dependent increase of calcium fluxes induced by β -amyloid peptides $A\beta_{1-42}$ and $A\beta_{25-35}$ in SH-SY5Y cells, suggesting a direct effect of the drug on amyloid channel formation. Molecular dynamics simulations gave structural insights into the role of cholesterol in amyloid channel formation and explained the inhibitory effect of bexarotene. Because it is the first drug that can both inhibit the binding of cholesterol to β -amyloid peptides and prevent calcium-permeable amyloid pore formation in the plasma membrane of neural cells, bexarotene might be considered as the prototype of a new class of anti-Alzheimer compounds. The experimental approach developed herein can be used as a screening strategy to identify such compounds.

KEYWORDS: Alzheimer's disease, amyloid, oligomers, cholesterol, bexarotene, therapy



Bexarotene, an anticancer drug, has recently been shown to restore some cognitive functions in animal models of Alzheimer's disease.¹ For this reason, bexarotene has logically been considered as a potential treatment for Alzheimer's disease.² However, the mechanism of action of this drug remains puzzling. In particular, the initially claimed effect of bexarotene on the reduction of amyloid plaques in brain tissues has not been confirmed.^{3–8} Nevertheless, two independent studies showed that bexarotene treatment could induce a significant reduction in the brain levels of soluble Alzheimer's peptide ($A\beta$).^{3,7} An effect of bexarotene on the clearance of $A\beta$ oligomers has also been observed.³ As for the effect of bexarotene on cognitive functions, conflicting results have been reported. Some authors noted an improvement of social recognition memory in bexarotene-treated APP/PS1 mice,⁶ whereas others, working with the same animal model, concluded that the drug failed to attenuate cognitive deficits.⁸ Hence, despite the hopes raised by the study published by Cramer et al.,¹ the usefulness of bexarotene as an anti-Alzheimer drug remains mostly uncertain. Therefore, as pointed out by LaClair et al.,⁸ further consideration of bexarotene for the therapy of Alzheimer's disease requires a

better understanding of its effects at the molecular and cellular levels.

In the search of a mechanism of action that would explain the beneficial effects of bexarotene in animal models of Alzheimer's disease, we focused our attention on the oligomerization process of β -amyloid peptides. Indeed, a growing line of evidence suggests that oligomers of amyloid proteins rather than amyloid plaques are the main molecular neurotoxic species in Alzheimer's disease.^{9–12} Moreover, Esparza et al. recently reported that, in a cohort of elderly patients, dementia symptoms correlated with the amount of $A\beta$ oligomers, whereas amyloid plaques were indiscriminately detected in Alzheimer's disease patients and in healthy individuals.¹³ Hence, disruption of amyloid plaques is no longer considered a therapeutic option for Alzheimer's disease. Instead, there is an emerging consensus on the necessity to identify new drugs that are capable of interfering with the formation of toxic oligomers.¹⁰ In this respect, some of the most toxic oligomers of $A\beta$ peptides are in fact embedded in the plasma membrane

Received: October 13, 2013

Revised: January 2, 2014

Published: January 2, 2014

of brain cells where they form calcium-permeable amyloid pores.^{9–11} Preventing the formation of these oligomers as well as disassembling preformed channels requires molecules to reach the lipid environment, a feature that is the prerogative of lipophilic and/or amphipathic molecules. It turns out that bexarotene is indeed an amphipathic compound that could potentially interact with membrane lipids. Among these lipids, cholesterol plays a central role because its concentration in the plasma membrane of neural cells is a key parameter that controls the neurotoxicity of $A\beta$ peptides.^{14,15} Indeed, cholesterol specifically interacts with monomeric $A\beta$ peptides,¹⁶ facilitates their insertion in the plasma membrane,¹⁷ and stimulates their functional oligomerization into calcium-permeable ion channels.^{15,18}

For all these reasons, we wondered if bexarotene, through its amphipathic properties, could in some ways interfere with a cholesterol-dependent effect involving $A\beta$ peptides in the lipid environment of the plasma membrane. In a recent study, our group has delineated the cholesterol-binding domain of $A\beta_{1-42}$ peptide to a contiguous domain encompassing residues 22–35.¹⁶ This cholesterol-binding domain contains the entire sequence of $A\beta_{25-35}$, a synthetic neurotoxic $A\beta$ peptide that has been widely used in experimental settings for studying the pathogenesis of Alzheimer's disease.^{19–21} Moreover, a slightly modified neurotoxic derivative of $A\beta_{25-35}$, referred to as [D-Ser²⁶] $A\beta_{25-35}$, is generated in the brain of Alzheimer patients after racemization of the Ser-26 residue of $A\beta_{1-40}$ followed by specific enzymatic cleavage.²² In the present study, we show that bexarotene shares structural analogy with cholesterol and competitively inhibits cholesterol binding to $A\beta_{25-35}$. We also show that bexarotene prevents the cholesterol-dependent oligomerization process of $A\beta_{1-42}$ and $A\beta_{25-35}$ peptides into calcium-permeable amyloid pores. Molecular dynamics simulations revealed insights into the formation of these amyloid channels in presence of cholesterol and their inhibition by bexarotene. Overall this study demonstrates a new mechanism of action for bexarotene and opens a promising therapeutic approach for Alzheimer's disease.

RESULTS

As a starting point of this study we have analyzed the chemical structure of bexarotene and observed that it shares interesting structural analogy with cholesterol (Figure 1A). Indeed, both bexarotene and cholesterol are amphipathic compounds, with a large apolar part consisting of a succession of hydrocarbon rings and a small polar headgroup (hydroxyl for cholesterol, carboxylate for bexarotene). Moreover, although cholesterol is slightly longer than bexarotene (respectively 17.0 and 13.5 Å), they have exactly the same width (6.5 Å). Overall, these structural features indicate that bexarotene can be considered as a cholesterol analogue (this is particularly obvious when both molecules are superposed).

Docking studies revealed that bexarotene and cholesterol interact with the same region located in C-terminal domain of $A\beta_{1-42}$ and share the same binding site on $A\beta_{25-35}$ (Figures 1B and 2). The amino group ($\epsilon\text{-NH}_3^+$) of Lys-28 can form either an electrostatic bond with the carboxylate group of bexarotene or a hydrogen bond with the OH group of cholesterol. The apolar parts of bexarotene and cholesterol interact with apolar residues (especially the isoleucine residues Ile-31 and Ile-32) through van der Waals contacts. Overall the energy of interaction between $A\beta_{25-35}$ and bexarotene was estimated to $-62.4 \text{ kJ}\cdot\text{mol}^{-1}$, which is significantly higher than the energy of

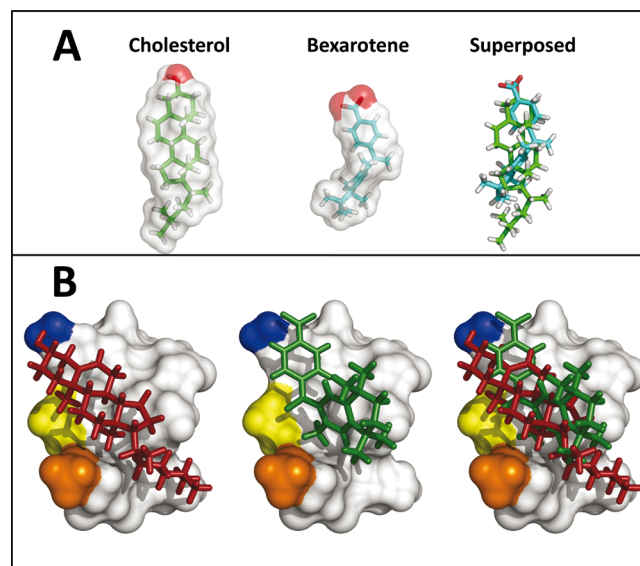


Figure 1. Cholesterol and bexarotene both interact with Alzheimer's β -amyloid peptide. (A) Both molecules display a similar architecture with a large apolar domain containing several rings and a small polar domain (hydroxyl group for cholesterol, carboxylate for bexarotene). Molecular surfaces are colored in white and oxygen atoms are highlighted in red. (B) Molecular docking of cholesterol (left panel) and bexarotene (middle panel) on $A\beta_{25-35}$. A superposition of both ligands on the peptide is shown in the right panel. Cholesterol is colored in red and bexarotene in green. The molecular surface of $A\beta_{25-35}$ is in white, Lys-28 in blue, Ile-31 in yellow, and Met-35 in orange.

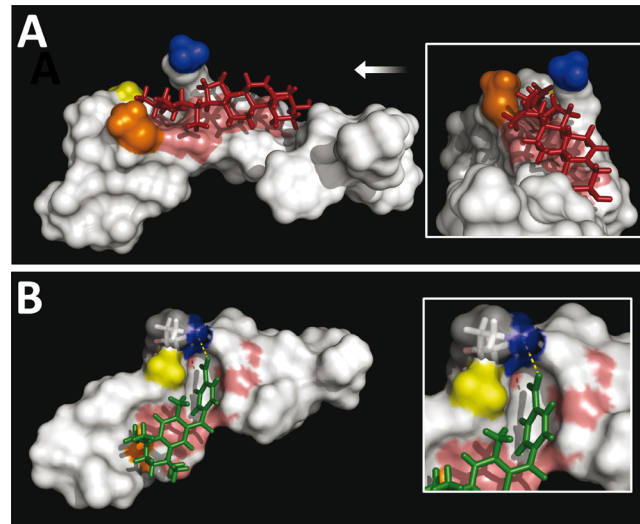


Figure 2. Docking of cholesterol and bexarotene on $A\beta_{1-42}$. Molecular docking of cholesterol (A) and bexarotene (B) on $A\beta_{1-42}$ was performed as indicated in the Methods section. To improve clarity, only the 17–40 region of the peptide is shown. Cholesterol is colored in red, and bexarotene in green. For the peptide, Lys-28 is in blue, Ile-31 is in yellow, and Met-35 is in orange. The electrostatic bond between bexarotene and Lys-28 is indicated by a yellow dotted line. Note that, during the course of the modeling process, bexarotene has drastically modified the structure of $A\beta_{1-42}$ so that the binding domain of cholesterol (colored in salmon) has been heavily distorted.

interaction of the cholesterol/ $A\beta_{25-35}$ complex ($-37.1 \text{ kJ}\cdot\text{mol}^{-1}$) (Table 1). It is important to note that Ser-26 is not involved in bexarotene binding, so that the drug could almost

Table 1. Energetics of Interaction of $\text{A}\beta$ Peptides with Cholesterol and Bexarotene

amino acid residue	$\text{A}\beta_{1-42}/\text{chol}$ (in vacuo) ^a	$\text{A}\beta_{1-42}/\text{bexa}$ (in vacuo) ^b	$\text{A}\beta_{25-35}/\text{chol}$ (in vacuo) ^c	$\text{A}\beta_{25-35}/\text{bexa}$ (in vacuo) ^c	$\text{A}\beta_{25-35}/\text{bexa}$ (in water) ^d	$[\text{D}-\text{Ser}^{26}]\text{A}\beta_{25-35}/\text{bexa}$ (in vacuo) ^e
Phe-20	-0.5					
Ala-21	-7.6					
Glu-22	-5.7					
Asp-23	-2.0					
Val-24	-16.1	-13.0				
Gly-25	-7.4	-4.8			-8.2	
Ser-26		-0.4				
Asn-27		-1.2		-4.2	-8.7	-4.4
Lys-28	-18.9	-12.0	-6.3	-25.4	-18.1	-26.4
Gly-29						
Ala-30		-2.5				
Ile-31	-9.7	-21.4	-15.3	-21.3	-18.5	-20.6
Ile-32	-3.6	-21.5	-3.1	-7.6	-9.2	-8.4
Gly-33						
Leu-34			-2.3			
Met-35	-5.3	-2.1	-10.1	-3.9	-4.2	-3.8
Val-36		-2.2				
Gly-37						
Gly-38						
Val-39						
Val-40		-2.3				
TOTAL	-76.8	-83.4	-37.1	-62.4	-66.9	-63.6

^aEstimation of the energy of interaction (ΔG , in $\text{kJ}\cdot\text{mol}^{-1}$) as determined by molecular docking of cholesterol on $\text{A}\beta_{1-42}$.¹⁶ ^bEstimation of the energy of interaction (ΔG , in $\text{kJ}\cdot\text{mol}^{-1}$) as determined by molecular docking of bexarotene on the C-terminal domain of $\text{A}\beta_{1-42}$ in the present study (Figure 2). ^cEnergy of interaction of the $\text{A}\beta_{25-35}/\text{cholesterol}$ and $\text{A}\beta_{25-35}/\text{bexarotene}$ complexes (Figure 1B). ^dEnergy of interaction calculated after molecular dynamics simulations of the $\text{A}\beta_{25-35}/\text{bexarotene}$ complex formed in presence of 450 water molecules. ^eEnergy of interaction of a $[\text{D}-\text{Ser}^{26}]\text{A}\beta_{25-35}/\text{bexarotene}$ complex.

indistinctively bind to the synthetic $\text{A}\beta_{25-35}$ peptide and to $[\text{D}-\text{Ser}^{26}]\text{A}\beta_{25-35}$, a neurotoxic peptide commonly found in the brain of Alzheimer patients.²² With the aim to validate this docking study, we analyzed the capacity of $\text{A}\beta$ fragments encompassing the 1–40 residues to interact with cholesterol and bexarotene (Figure 3). In this study, stable monolayers of cholesterol or bexarotene were prepared at the air–water interface, after which the peptide was injected in the aqueous subphase. This Langmuir setup allowed us to follow the interaction of a peptide with a lipid, by measuring in real-time the peptide-induced changes in the surface pressure of the monolayer.²³ This ultrasensitive technique requires ultrapure compounds devoid of surfactant contaminants that could nonspecifically affect the surface pressure. For these reasons we carefully checked the purity of bexarotene and cholesterol by spectrophotometry and high performance thin layer chromatography (Figure 3). The spectrum of absorbance of bexarotene indicated a single peak with a maximal absorption at 264 nm (Figure 3A), corresponding to the expected λ_{\max} of the compound.²⁴ The chromatographic behavior of bexarotene and cholesterol (Figure 3B) also revealed in each case a unique molecular species without any detectable contaminant. In particular, oxidized cholesterol was totally absent from our cholesterol solution. These physicochemical characterizations validated the use of Langmuir monolayers for studying the interaction of $\text{A}\beta$ peptides with cholesterol and bexarotene. The kinetics studies in Figure 3C and D showed that both cholesterol and bexarotene physically interact with the C-terminal domain of $\text{A}\beta$ (fragment 17–40) but not with the N-terminal domain (fragment 1–16). This is consistent with our docking study that identified the 25–35 region of the C-terminal domain of $\text{A}\beta_{1-42}$ as a common cholesterol/

bexarotene binding site. The interaction of bexarotene with $\text{A}\beta_{25-35}$ is shown in Figure 4A. In this experiment, several bexarotene monolayers were prepared at various values of the initial pressure, the higher pressures corresponding to condensed monolayers with high amounts of bexarotene. After equilibration, the $\text{A}\beta_{25-35}$ peptide was injected in the aqueous subphase and its interaction with bexarotene was evidenced by an increase in the surface pressure. The initial velocity (v_i) of the interaction between $\text{A}\beta_{25-35}$ and bexarotene was determined for each monolayer. The data showed that v_i gradually decreased as the initial surface pressure of the bexarotene monolayer increased. This is typical of an insertion process that becomes less effective as the number of lipid molecules in the monolayer increases.²⁵ Thus, these data indicated that the peptide was not loosely adsorbed at the surface of the bexarotene monolayer but did penetrate the monolayer to fully interact with the drug, in agreement with our molecular modeling studies. (Figure 1B).

The next step was to evaluate the capacity of bexarotene to inhibit the binding of cholesterol to the $\text{A}\beta_{25-35}$ peptide. In this experiment, a monolayer of cholesterol was spread at the air–water interface, and the peptide was injected in the aqueous subphase. The insertion of the peptide within the cholesterol monolayer was measured by a real-time increase of the surface pressure.²⁵ When bexarotene was injected in the subphase prior to $\text{A}\beta_{25-35}$, the peptide could no longer interact with cholesterol (Figure 4B). A molecular bexarotene/peptide ratio of 1:3 was sufficient to totally prevent the interaction between cholesterol and $\text{A}\beta_{25-35}$. This is in full agreement with our docking study which indicated a higher affinity of $\text{A}\beta_{25-35}$ for bexarotene compared with cholesterol. These data demonstrated that bexarotene binds to $\text{A}\beta_{25-35}$ in the aqueous phase and

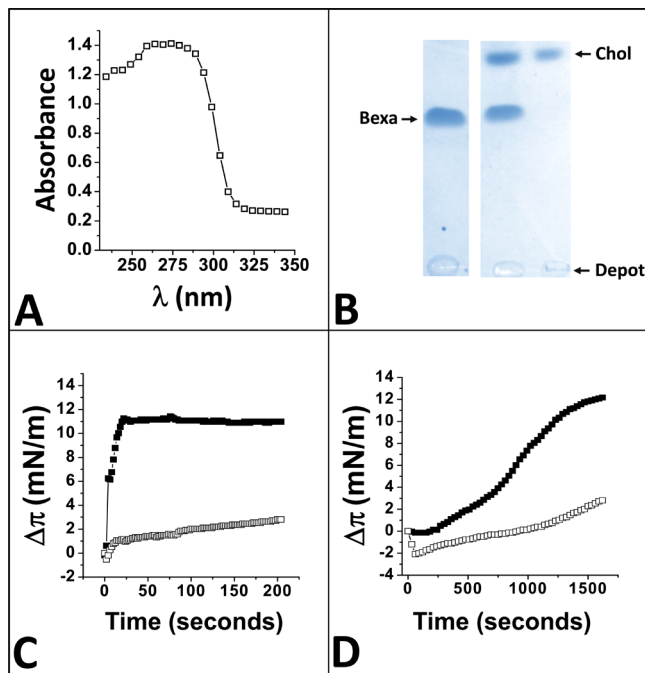


Figure 3. Physicochemical studies of the interaction between Alzheimer's peptides and cholesterol or bexarotene. (A) Absorption spectrum of bexarotene showing a single peak with a maximum at 264 nm. (B) High performance thin layer chromatography of bexarotene (left lane), cholesterol (right lane), and a 1:1 (mol:mol) mixture of both molecules (middle lane). (C, D) Time course of interaction between Alzheimer's peptides and cholesterol or bexarotene. Cholesterol monolayers (C) were prepared by depositing a drop of cholesterol ($0.25 \text{ mg}\cdot\text{mL}^{-1}$) at the surface of a phosphate buffer subphase. Stable monolayers of bexarotene (D) were prepared by injecting $2 \mu\text{L}$ of ethanolic bexarotene ($1 \text{ mg}\cdot\text{mL}^{-1}$) in $800 \mu\text{L}$ of phosphate buffer 50 mM at pH 6.3. After equilibration of each monolayer, the indicated peptide was injected in the subphase at a final concentration of $10 \mu\text{M}$. In both panels, the data show the surface pressure changes induced by $A\beta_{1-16}$ (open squares) or $A\beta_{17-40}$ (full squares). All experiments were performed in triplicate, and one representative curve is shown for each peptide (SD < 15%).

competitively inhibits its insertion within the cholesterol monolayer. Extrapolated to the *in vivo* situation, this suggests that bexarotene could restrict the insertion of $A\beta_{25-35}$ into cholesterol-rich domains of the plasma membrane of neural cells. Molecular dynamics simulations confirmed that bexarotene could interact with $A\beta_{25-35}$ in a water environment (Figure 5A). Yet, in this case, the carboxylate group of bexarotene did not interact with the $\epsilon\text{-NH}_3^+$ group of Lys-28, but instead formed a hydrogen bond with the $\alpha\text{-NH}$ group of Gly-25 (Figure 5B). Indeed, a network of water molecules surrounding the cationic group of Lys-28 moved the carboxylate group at a distance of 4.6 \AA (Figure 5C). This structural rearrangement brought the carboxylate at only 3.0 \AA of the $\alpha\text{-NH}$ group of Gly-25, consistent with the formation of a new hydrogen bond (Figure 5D). Most importantly, when water molecules were removed and the simulations again performed in vacuo, the carboxylate group of bexarotene lefted Gly-25 and restored its electrostatic bond with Lys-28 (Figure 5E and F). The energy of interaction of the bexarotene/ $A\beta_{25-35}$ complex in water was estimated to $-66.9 \text{ kJ}\cdot\text{mol}^{-1}$, a value slightly higher to the one obtained in vacuo (Table 1). Thus, these data strongly support the notion that bexarotene is able to interact with $A\beta_{25-35}$ both in an apolar milieu (in vacuo

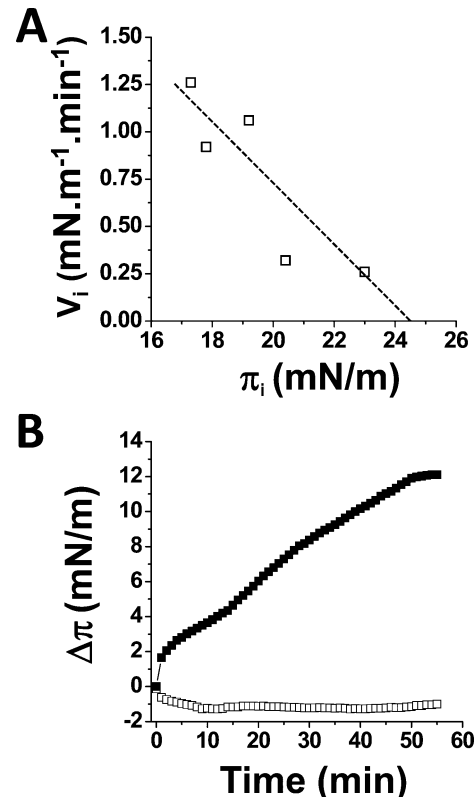


Figure 4. Cholesterol binding to $A\beta_{25-35}$ is competitively inhibited by bexarotene. (A) Bexarotene specifically interacts with $A\beta_{25-35}$. Stable monolayers of bexarotene were prepared at various values of the initial surface pressure π_i . The $A\beta_{25-35}$ peptide ($10 \mu\text{M}$) was then injected in the aqueous subphase and the initial velocity of the interaction was determined for each π_i value. (B) The data show the interaction of $A\beta_{25-35}$ with a monolayer of cholesterol. After the equilibrium of the cholesterol monolayer (usually within 1–2 min), $0.5 \mu\text{L}$ of ethanol either not containing (full squares) or containing bexarotene (open squares) was injected in the subphase. After 30 s of equilibration, the peptide was injected in the subphase at a final concentration of $10 \mu\text{M}$. The bexarotene/peptide molar ratio is 1:3. All experiments were performed in triplicate, and one representative curve is shown for each peptide (SD < 15%).

conditions of Figure 1B) and in an aqueous environment (modeling studies in presence of water molecules, Figure 5A).

Since the membrane insertion of $A\beta$ peptides can lead to the formation of calcium-permeable amyloid pores,^{11,26} we investigated the effect of bexarotene on this process. To this end, we have followed Ca^{2+} exchanges in neuroblastoma SH-SY5Y cells loaded with the fluorescent-sensitive dye Fluo-4 AM and subsequently treated with $A\beta_{25-35}$ or $A\beta_{1-42}$ (Figure 6). The data in Figure 6A (left panel) show that when added to cells bathed in Ca^{2+} -containing buffer, $A\beta_{25-35}$ induced a progressive, time-dependent increase of intracellular Ca^{2+} levels (black curve). This elevation of Ca^{2+} levels induced by $A\beta_{25-35}$ was no longer observed in presence of Zn^{2+} , a classical amyloid channel inhibitor²⁷ (Figure 6A, left panel, red curve). These data indicated that the Ca^{2+} fluxes are mediated by bona fide amyloid pores formed by oligomeric $A\beta_{25-35}$ peptides, and not by nonspecific membrane damage. To determine if these amyloid pores require cholesterol, we treated SH-SY5Y cells with a nontoxic concentration of the cholesterol depleting agent methyl- β -cyclodextrin. After 24 h of incubation, the cells were washed, loaded with Fluo-4 AM, and treated with $A\beta_{25-35}$.

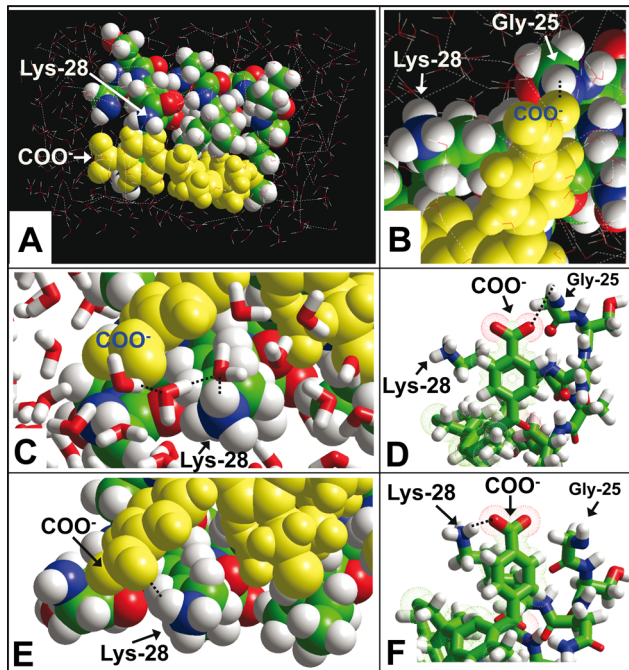


Figure 5. Molecular modeling of bexarotene/A β _{25–35} interactions in vacuo and in water. (A) Molecular dynamics simulations of a bexarotene/A β _{25–35} complex with 450 water molecules in a 12 000 Å³ volume (20 × 20 × 30 Å³). Bexarotene is in yellow, the peptide in atom colors, and water molecules in sticks. Hydrogen bonds are indicated with white dotted lines. (B) Same model as in (A) at a higher magnification. The carboxylate group of bexarotene forms a hydrogen bond with the NH₂-terminal group of Gly-25. Thus, in a bexarotene/A β _{1–42} complex, the hydrogen bond would involve the peptidic NH group linking Val-24 and Gly-25. (C) Network of hydrogen bonds of water molecules located between the carboxylate group of bexarotene and the ε-NH₃⁺ of Lys-28 in A β _{25–35}. This intercalation of water molecules breaks the electrostatic bond linking bexarotene and Lys-28. (D) The water-driven reorientation of A β _{25–35} side chains switches the carboxylate group of bexarotene which does no longer bind to Lys-28 but now interacts with the NH₂-terminal group of Gly-25. To improve clarity, water molecules are not represented and only one hydrogen atom of the N-terminal amino group of the peptide is shown. In this complex, the carboxylate group of bexarotene is at 4.6 Å of the ε-NH₃⁺ of Lys-28 and at 3.0 Å of the NH group of Gly-25. (E, F) When water molecules were removed from the simulation box, the complex spontaneously evolved toward the reformation of an electrostatic bond linking the carboxylate group of bexarotene and Lys-28, whereas Gly-25 was again rejected at the periphery of the complex. In this case, the carboxylate group of bexarotene is at 2.6 Å of the ε-NH₃⁺ of Lys-28 and at 4.8 Å of the NH group of Gly-25.

As shown in Figure 6A (middle panel), the methyl- β -cyclodextrin treatment (red curve) abolished the elevation of Ca²⁺ entry induced by the A β _{25–35} peptide. Thus, the oligomerization of A β _{25–35} peptides into functional amyloid pores is a cholesterol-dependent process, in full agreement with previous data obtained with A β _{22–35} and A β _{1–42} peptides.¹⁸ Finally, when the cells were treated with A β _{25–35} in presence of bexarotene (molar ratio 1:1), no increase in Ca²⁺ fluxes could be observed (Figure 6A, right panel). This strong inhibitory effect of bexarotene on amyloid pore function was reproducibly observed under various experimental conditions, i.e. preincubation of bexarotene and A β _{25–35} for 1 h (blue curve) or simultaneous addition of both compounds onto the cells (red curve). Overall, these data showed that bexarotene interacts

with A β _{25–35}, occupies the cholesterol-binding site, inhibits the insertion of A β _{25–35} within cholesterol-rich domains (mimicked by cholesterol monolayers), and abolishes the elevation of Ca²⁺ fluxes generated by cholesterol-dependent and Zn²⁺-sensitive amyloid pores formed by A β _{25–35}. Bexarotene could also inhibit the elevation of Ca²⁺ entry induced by the full-length A β _{1–42} peptide, at a bexarotene/peptide molar ratio of 1:1 (Figure 6B, left panel). As for A β _{25–35}, the inhibitory effect was obtained when bexarotene and A β _{1–42} were preincubated for 1 h (blue curve) or simultaneously added onto the cells (red curve). The photomicrographs taken during this experiment proved that most of the cells responded to bexarotene (Figure 6B, right panel). The histograms in Figure 6C showed that, after 1 h of incubation, the Ca²⁺ fluxes generated by both A β _{25–35} and A β _{1–42} were significantly decreased by bexarotene.

Molecular dynamics simulations were conducted to figure out how A β _{25–35} peptides could form oligomeric channels in cholesterol-containing membranes (Figure 7). To this end, several monomers of A β _{25–35} peptide in complex with cholesterol were introduced in a phospholipid matrix. Several types of oligomers could be formed under these conditions (e.g., tetramers), especially the formation of a regular annular channel consisting of 8 A β /cholesterol units. This channel was further stabilized by eight supplementary cholesterol molecules that filled the remaining gap between the peptides and surrounding membrane phospholipids. Thus, the actual stoichiometry of the channel is A β ₈/cholesterol₁₆ (Figure 7A). The tilted geometry of each individual cholesterol/A β _{25–35} complex allows the formation of efficient van der Waals contacts between two vicinal peptides. Such van der Waals interactions involve residues Gly-25, Asn-27, and Ile-31 on one peptide, and Ser-26, Gly-29, and Gly-33 on its immediate neighbor. In this respect, the A β _{25–35} channel should be distinguished from the longer A β _{22–35} channel recently analyzed by our group,¹⁸ the latter being stabilized by only eight cholesterol molecules and a hydrogen bond linking Asn-27 and Lys-28 of two vicinal peptide units.

Nevertheless, both the pore and outer diameters of the A β _{25–35} channel (respectively 1.5 and 4.8 nm) are compatible with the values obtained with various Alzheimer's peptides on the basis of both in silico and atomic force microscopy approaches.^{18,26} As shown in Figure 7B (upper panel), the pore mouth is delineated by a circular arrangement of the eight serine residues (Ser-26) whose side chain hydroxyl groups form an attractive crater for Ca²⁺ ions.

Interestingly, molecular modeling studies also indicate that Zn²⁺ ions can bind to these hydroxyl groups (Figure 7B lower panel). Such coordination complexes between Zn²⁺ and Ser residues have been characterized in cocatalytic zinc binding sites of enzymes such as *E. coli* alkaline phosphatase.²⁸ It can be seen that the presence of Zn²⁺ ions bound to Ser-26 residues restricts the accessibility of Ca²⁺ ions to the channel, consistent with the data of Figure 6A.

DISCUSSION

In this report, we describe a new mechanism of action of bexarotene, a drug which has been recently reported to improve cognitive functions in animal models of Alzheimer's disease.¹ Unfortunately, the usefulness of bexarotene as a therapy for Alzheimer's disease has been questioned, especially because the effects of bexarotene on the clearance of amyloid plaques could not be reproduced.^{3–8} However, some studies still suggest that the drug may stimulate the clearance of soluble A β monomers

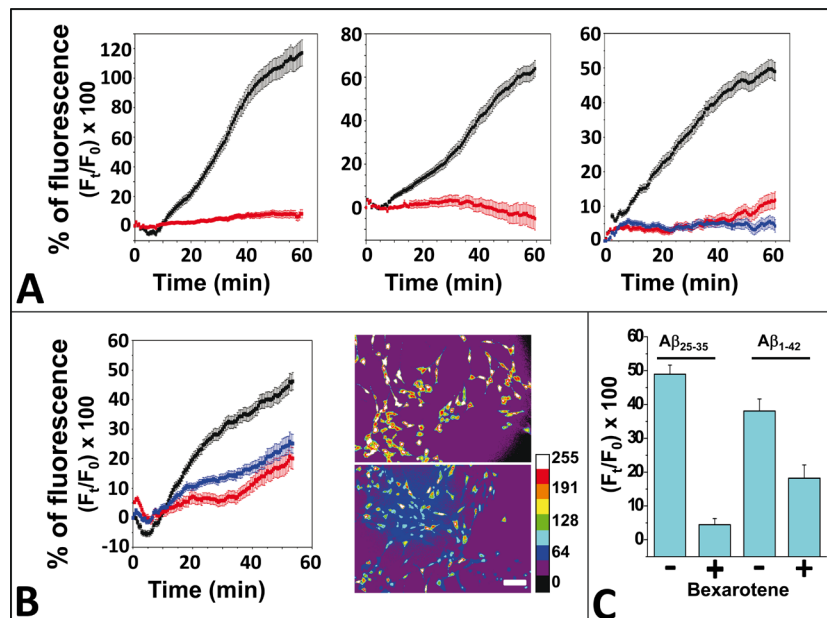


Figure 6. Cholesterol-dependent calcium amyloid channel formation and its inhibition by bexarotene. (A) Left panel: $\text{A}\beta_{25-35}$ calcium increase is inhibited by Zn²⁺. During loading with Ca²⁺ indicator (Fluo-4 AM), SH-SY5Y cells were treated (red; $n = 60$) or not (black; $n = 60$) with Zn²⁺ (50 μ M). The cells were then treated with $\text{A}\beta_{25-35}$ peptide (220 nM), and Ca²⁺ dependent fluorescence was analyzed. Signals were expressed as fluorescence after treatment (F_t) divided by the fluorescence before treatment (F_0) and multiplied by 100. Middle panel: $\text{A}\beta_{25-35}$ calcium increase is cholesterol-dependent. SH-SY5Y cells were either pretreated (red; $n = 76$) or not by methyl- β -cyclodextrin (black; $n = 81$), and the $\text{A}\beta_{25-35}$ effect was evaluated by calcium measurements. Right panel: bexarotene inhibits $\text{A}\beta_{25-35}$ calcium elevation. $\text{A}\beta_{25-35}$ and bexarotene (both 220 nM) were mixed extemporaneously and either directly injected onto the cells or preincubated for 1 h before injection. Cells were treated with $\text{A}\beta_{25-35}$ alone (black; $n = 190$), $\text{A}\beta_{25-35}$ /bexarotene not preincubated (red; $n = 170$) or $\text{A}\beta_{25-35}$ /bexarotene preincubated (blue; $n = 184$). (B) Left panel: bexarotene reduces $\text{A}\beta_{1-42}$ calcium elevation. $\text{A}\beta_{1-42}$ and bexarotene (both 220 nM) were mixed extemporaneously and either directly injected onto the cells or preincubated for 1 h before injection. Cells were treated with 220 nM of $\text{A}\beta_{1-42}$ alone (black; $n = 120$), $\text{A}\beta_{1-42}$ /bexarotene not preincubated (red; $n = 90$), or $\text{A}\beta_{1-42}$ /bexarotene preincubated (blue; $n = 80$), and Ca²⁺ dependent fluorescence was measured. The images show pseudocolor representations of cells (scale bar: 100 μ m). The upper micrograph shows the cells treated with $\text{A}\beta_{1-42}$ alone (corresponding to the black curve), and the lower one shows the cells treated with the $\text{A}\beta_{1-42}$ /bexarotene mixture (corresponding to the blue curve). Warmer colors correspond to higher fluorescence. (C) Inhibitory effects of bexarotene on the calcium fluxes elicited by $\text{A}\beta_{25-35}$ and $\text{A}\beta_{1-42}$ after 1 h of incubation (calculated from black and blue curves in (A) and (B)). All quantitative data in (A)–(C) panels are mean \pm SD.

and/or oligomers.^{3,7} This may indicate that the mechanism of action of bexarotene is not the one initially postulated, that is, an apolipoprotein-E-mediated clearance of amyloid plaques via microglial cells.^{1,4} Given the potential therapeutic interest of bexarotene, we looked for an alternative mechanism. First, it is worthy of note that our initial interest in bexarotene was based on its chemical structure which presents interesting analogies with cholesterol (Figure 1A). To the best of our knowledge, this feature has not been previously highlighted in the literature. Moreover, we have recently identified, in the C-terminal domain of $\text{A}\beta_{1-42}$, a functional cholesterol binding domain¹⁶ that appeared to play a critical role in the oligomerization of $\text{A}\beta$ peptides into neurotoxic calcium channels in the plasma membrane of neural cells.¹⁸ These data prompted us to determine whether bexarotene, now considered as a “cholesterol analogue”, could occupy the cholesterol-binding site of $\text{A}\beta$ peptides and thus function as a competitive inhibitor of the cholesterol/ $\text{A}\beta$ interaction.

To answer this question, we designed a functional assay aimed at measuring the interaction of bexarotene with various $\text{A}\beta$ peptides. In this assay, a monolayer of bexarotene was prepared at the air–water interface and probed with $\text{A}\beta$ peptides added in the aqueous subphase. The interaction was then quantified by measuring in real-time the peptide-induced increases in the surface pressure (Figure 3D). The monolayer system could also be used as a competition assay for studying

the ability of bexarotene to bind to $\text{A}\beta$ peptides in the aqueous phase and inhibit the insertion of these peptides in the cholesterol monolayer (Figure 4B). With this experimental setup we first demonstrated that bexarotene specifically interacts with the C-terminal domain of $\text{A}\beta_{1-42}$, just like cholesterol does (Figure 3C). More precisely, both cholesterol and bexarotene could bind to $\text{A}\beta_{25-35}$, a minimal neurotoxic $\text{A}\beta$ peptide.²¹ With the monolayer system in the competition setting mode, we showed that bexarotene can also bind to $\text{A}\beta_{25-35}$ in the aqueous phase and efficiently prevent the insertion of the peptide within the cholesterol-containing monolayer (Figure 4). Finally we showed that $\text{A}\beta_{25-35}$ could form cholesterol-dependent, zinc-sensitive calcium channels in neural cells and that bexarotene could block the formation of these channels (Figure 6). Taken together, these data demonstrated that bexarotene can inhibit the binding of cholesterol to $\text{A}\beta_{25-35}$ (and probably to any neurotoxic $\text{A}\beta$ peptide containing the 25–35 motif, including $\text{A}\beta_{1-40}$, $\text{A}\beta_{1-42}$ as well as truncated $\text{A}\beta$ species such as $\text{A}\beta_{22-35}$, [D-Ser²⁶] $\text{A}\beta_{25-35}$,²¹ or $\text{A}\beta_{17-40/42}$ (p3 peptides).²⁶ The possibility that bexarotene could bind to p3 peptides in vivo is of interest because, although nonamyloidogenic, these peptides can indeed form oligomeric calcium channels in the plasma membrane of neural cells.²⁶ Thus, it will be important to evaluate the protective effect of bexarotene against p3-induced neurotoxicity. In any case, our data showed that the oligomerization

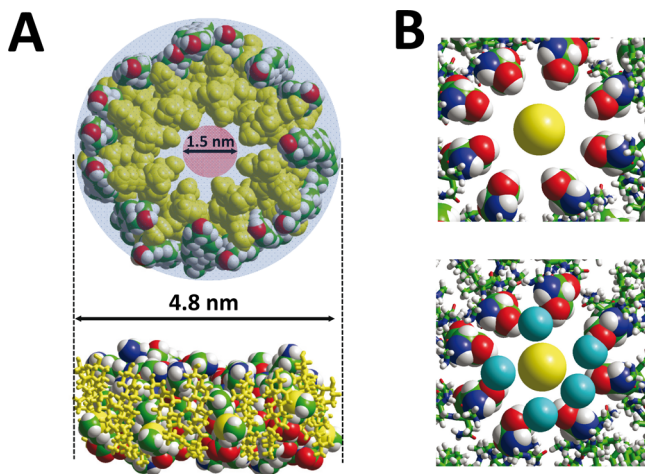


Figure 7. Model of an annular channel formed by 8 units of $\text{A}\beta_{25-35}$ and 16 molecules of cholesterol. (A) The association of 8 $\text{A}\beta_{25-35}$ peptides (colored in yellow) forms a regular annular structure with a central pore (upper panel). This annular channel is stabilized by 16 cholesterol molecules (atom colors are green for carbon, red for oxygen, and gray for hydrogen). A side view of the channel is shown at the same scale below the annular model (cholesterol in yellow, atom colors for the peptides). (B) Binding of Zn^{2+} cations to Ser-26 of the $\text{A}\beta_{25-35}$ /cholesterol channel. The oxygen atoms of the eight Ser-26 residues (upper model, atoms colored in red) form a perfect ring of partial negative charges able to attract calcium ions. A Ca^{2+} ion (in yellow) has been placed at the center of the pore mouth of the channel. The coordination of 5 Zn^{2+} cations (in cyan) with the oxygen atoms of the hydroxyl groups of Ser-26 is shown in the lower panel.

of $\text{A}\beta_{25-35}$ into amyloid pores is a cholesterol-dependent process, and that bexarotene can prevent the formation of these toxic oligomers. A model of the cholesterol/ $\text{A}\beta_{25-35}$ channel obtained by means of molecular dynamics simulations (Figure 7) confirmed the key role of cholesterol in the oligomeric organization of $\text{A}\beta_{25-35}$ in a cholesterol-rich domain. Specifically, this model explains (i) why the calcium fluxes induced by $\text{A}\beta_{25-35}$ are no longer observed in cholesterol-depleted cells, and (ii) why bexarotene, which inhibits the binding of cholesterol to $\text{A}\beta_{25-35}$ in both water and membrane environments, prevents the formation of functional oligomeric channels. In the same way, we have previously demonstrated that the pathologically relevant $\text{A}\beta_{1-42}$ peptide forms cholesterol-dependent calcium channels in SH-SY5Y cells.¹⁸ Our molecular modeling studies (Figure 2) indicate that bexarotene could interact with $\text{A}\beta_{1-42}$ and thus prevent cholesterol binding to this peptide. In line with these data, we found that bexarotene could also decrease the calcium fluxes induced by oligomeric $\text{A}\beta_{1-42}$ channels (Figure 6). Thus, the ability of bexarotene to interfere with amyloid pore formation also applies to a major neurotoxic $\text{A}\beta$ peptide that is abundantly expressed in the brain of Alzheimer's disease patients.

CONCLUSION AND PERSPECTIVES

The present study stands at the crossroads of two distinct but converging fields of investigation. On one hand, amyloid oligomers instead of plaques are currently being recognized as the main toxic molecular species that contributes to the pathogenesis of Alzheimer's disease.^{9–13} On the other hand, a growing line of evidence suggests that cholesterol, a key epidemiological cofactor of Alzheimer's disease,²⁹ interacts with $\text{A}\beta$ peptides,¹⁶ and facilitates both their membrane inser-

tion^{17,30} and the formation of oligomeric amyloid pores.^{18,31,32} Unfortunately, this progress in our comprehension of the role of cholesterol in Alzheimer's disease has not yet led to new therapeutic strategies, apart from the use of statins to decrease plasma cholesterol levels.²⁹ Because it mimics cholesterol and prevents cholesterol-induced neurotoxic effects of β -amyloid peptide oligomers, bexarotene fills this gap and should thus be considered as the prototype of a new cholesterol-triggered therapeutic option for Alzheimer's and probably other cholesterol-linked neurodegenerative diseases.^{9,33} Its effect is rapid (less than 1 h for cholesterol binding and for obtaining a total inhibition of amyloid channel formation in cultured cells), which is consistent with the rapid recovery of cognitive functions observed with animal models of Alzheimer's disease.¹ Alternatively, the ability of bexarotene to bind to $\text{A}\beta$ peptides in solution (Figures 4 and 5) could explain why the drug stimulates the clearance of soluble $\text{A}\beta$ from the brain of animal models of Alzheimer's disease.^{1,3,4,7} Yet it is likely that the main effect of bexarotene is to block amyloid channel formation. As an amphipathic molecule, this drug can easily penetrate the plasma membrane. As a cholesterol-like compound, it can occupy the cholesterol-binding domain of $\text{A}\beta$. Because of its high affinity with this cholesterol-binding domain, it can prevent $\text{A}\beta$ peptides to interact with cholesterol and displace cholesterol molecules already bound to the peptides. Since amyloid pores do not function in absence of cholesterol (Figure 6), this would cure "peptide-infected cells"^{9,10,25} through an inhibition of ion channel formation and/or function. Therapies based on the disruption of amyloid plaques have failed so far.³⁴ For this reason, it is of high interest to discover new drugs capable of reaching membrane-embedded toxic oligomers and perturb their association with cholesterol.¹⁰ The experimental approach developed herein can serve as a simple, rapid, and low-cost screening strategy to identify such cholesterol/ $\text{A}\beta$ breakers at the preclinical level.

METHODS

Materials. Synthetic peptides were purchased from rPeptide (Bogart, GA) and Schafer-N, (Copenhagen, Denmark). Cholesterol was from Matreya (Pleasant Gap, PA), and bexarotene from Cayman Chemicals (San Antonio, TX). The purity of bexarotene and cholesterol was assessed by high performance thin layer chromatography (HPTLC) using HPTLC silica gel 60 plates (#1.05547.0001, Merck, Whitehouse Station, NJ). Lipids were developed with chloroform/methanol (50:5, vol/vol) and colored with Coomassie brilliant blue R250 (Sigma, St. Louis, MO).

In Silico Studies. Molecular docking and molecular dynamics simulations were performed with the Hyperchem 8 program (ChemCAD, Obernay, France) as previously described.^{16,18,25} Briefly, geometry optimization of peptide/cholesterol and peptide/bexarotene complexes was achieved using the unconstrained optimization rendered by the Polak-Ribière conjugate gradient algorithm. Molecular dynamics simulations were then performed for iterative periods of times of 1 ns in vacuo with the Bio+ (CHARMM) force field.^{35,36} The energies of interaction were estimated with the Molegro Molecular Viewer.³⁷ The molecular models in Figures 1 and 2 have been prepared with the PyMOL Molecular Graphics System, version 1.2r3pre, Schrödinger, LLC.

Physicochemical Studies. Peptide–cholesterol and peptide–bexarotene interactions were measured at the air–water interface with the Microtrough device (Kibron Inc.) as described previously.^{16,38}

Cell Culture. Neuroblastoma SH-SY5Y cells obtained from the ATCC were grown at 37 °C with 5% CO_2 in DMEM/F12 medium supplemented with 10% fetal calf serum. Methyl- β -cyclodextrin treatment of SH-SY5Y cells (1 mM for 24 h) was performed as previously described.¹⁸

Calcium Measurements. Cells were plated in 35 mm culture dishes, grown during 72 h and loaded with 5 μ M Fluo-4 AM (Invitrogen-Life Technologies, Saint Aubin, France) for 30 min in the dark, washed three times with HBSS (Gibco-Life Technologies, Saint Aubin, France), and incubated for 20 min at 37 °C. The calcium fluxes were estimated by measuring the variation of cell fluorescence intensity after peptide injection into the recording chamber directly above an upright microscope objective (BX51W Olympus, Rungis, France) equipped with an illuminator system MT20 module.¹⁸ Fluorescence emission at 525 nm was imaged by a digital camera CDD (ORCA-ER Hamanatsu, Japan) after fluorescence excitation at 490 nm. Times-lapse images (1 frame/10 s) were collected using the CellR Software (Olympus). Signals were expressed as fluorescence after treatment (F_t) divided by the fluorescence before treatment (F_0) multiplied by 100. The results are averaged and the percentage of fluorescence of control is subtracted for each value.

AUTHOR INFORMATION

Corresponding Author

*Mailing address: EA-4674, Interactions Moléculaires et Systèmes Membranaires, Université d'Aix-Marseille, Faculté des Sciences Saint-Jérôme, Avenue Escadrille Normandie-Niemen, Service 331, 13013 Marseille, France. Tel: +33 491 288 761. E-mail: jacques.fantini@univ-amu.fr

Author Contributions

J. Fantini, N. Garmy, and N. Yahi planned the study, performed the modeling simulations, and wrote the article; C. Di Scala, J. D. Troadec, K. Sadelli, and H. Chahinian performed the calcium flux studies and analyzed the data; N. Yahi performed the monolayer experiments and analyzed the data.

Notes

The authors declare no competing financial interest.

REFERENCES

- (1) Cramer, P. E., Cirrito, J. R., Wesson, D. W., Lee, C. Y., Karlo, J. C., Zinn, A. E., Casali, B. T., Restivo, J. L., Goebel, W. D., James, M. J., Brunden, K. R., Wilson, D. A., and Landreth, G. E. (2012) ApoE-directed therapeutics rapidly clear β -amyloid and reverse deficits in AD mouse models. *Science* 335, 1503–1506.
- (2) LaFerla, F. M. (2012) Preclinical success against Alzheimer's disease with an old drug. *N. Engl. J. Med.* 367, 570–572.
- (3) Fitz, N. F., Cronican, A. A., Lefterov, I., and Koldamova, R. (2013) Comment on "ApoE-Directed Therapeutics Rapidly Clear β -Amyloid and Reverse Deficits in AD Mouse Models". *Science* 340, 924-c–.
- (4) Landreth, G. E., Cramer, P. E., Lakner, M. M., Cirrito, J. R., Wesson, D. W., Brunden, K. R., and Wilson, D. A. (2013) Response to Comments on "ApoE-Directed Therapeutics Rapidly Clear β -Amyloid and Reverse Deficits in AD Mouse Models". *Science* 340, 924-g–.
- (5) Price, A. R., Xu, G., Siemienksi, Z. B., Smithson, L. A., Borchelt, D. R., Golde, T. E., and Felsenstein, K. M. (2013) Comment on "ApoE-Directed Therapeutics Rapidly Clear β -Amyloid and Reverse Deficits in AD Mouse Models". *Science* 340, 924-d–.
- (6) Tessier, I., Lo, A. C., Roberfroid, A., Dietvorst, S., Van Broeck, B., Borgers, M., Gijsen, H., Moechars, D., Mercken, M., Kemp, J., D'Hooge, R., and De Strooper, B. (2013) Comment on "ApoE-Directed Therapeutics Rapidly Clear β -Amyloid and Reverse Deficits in AD Mouse Models". *Science* 340, 924-e–.
- (7) Veeraraghavalu, K., Zhang, C., Miller, S., Hefendehl, J. K., Rajapaksha, T. W., Ulrich, J., Jucker, M., Holtzman, D. M., Tanzi, R. E., Vassar, R., and Sisodia, S. S. (2013) Comment on "ApoE-Directed Therapeutics Rapidly Clear β -Amyloid and Reverse Deficits in AD Mouse Models". *Science* 340, 924-f–.
- (8) LaClair, K. D., Manaye, K. F., Lee, D. L., Allard, J. S., Savonenko, A. V., Troncoso, J. C., and Wong, P. C. (2013) Treatment with bexarotene, a compound that increases apolipoprotein-E, provides no cognitive benefit in mutant APP/PS1 mice. *Mol. Neurodegener.* 8, 18.
- (9) Fantini, J., and Yahi, N. (2010) Molecular insights into amyloid regulation by membrane cholesterol and sphingolipids: common mechanisms in neurodegenerative diseases. *Expert Rev. Mol. Med.* 12, e27.
- (10) Jang, H., Connelly, L., Arce, F. T., Ramachandran, R., Lal, R., Kagan, B. L., and Nussinov, R. (2013) Alzheimer's disease: which type of amyloid-preventing drug agents to employ? *Phys. Chem. Chem. Phys.* 15, 8868–8877.
- (11) Demuro, A., Mina, E., Kayed, R., Milton, S. C., Parker, I., and Glabe, C. G. (2005) Calcium dysregulation and membrane disruption as a ubiquitous neurotoxic mechanism of soluble amyloid oligomers. *J. Biol. Chem.* 280, 17294–17300.
- (12) Kayed, R., and Lasagna-Reeves, C. A. (2013) Molecular mechanisms of amyloid oligomers toxicity. *J. Alzheimer's Dis.* 33, S67–S78.
- (13) Esparza, T. J., Zhao, H., Cirrito, J. R., Cairns, N. J., Bateman, R. J., Holtzman, D. M., and Brody, D. L. (2012) Amyloid-beta oligomerization in Alzheimer dementia versus high-pathology controls. *Ann. Neurol.* 73, 104–119.
- (14) Arispe, N., and Doh, M. (2002) Plasma membrane cholesterol controls the cytotoxicity of Alzheimer's disease AbetaP (1–40) and (1–42) peptides. *FASEB J.* 16, 1526–1536.
- (15) Abramov, A. Y., Ionov, M., Pavlov, E., and Duchen, M. R. (2011) Membrane cholesterol content plays a key role in the neurotoxicity of β -amyloid: implications for Alzheimer's disease. *Aging Cell* 10, 595–603.
- (16) Di Scala, C., Yahi, N., Lelièvre, C., Garmy, N., Chahinian, H., and Fantini, J. (2013) Biochemical identification of a linear cholesterol-binding domain within Alzheimer's β amyloid peptide. *ACS Chem. Neurosci.* 4, 509–517.
- (17) Yu, X., and Zheng, J. (2012) Cholesterol promotes the interaction of Alzheimer β -amyloid monomer with lipid bilayer. *J. Mol. Biol.* 421, 561–571.
- (18) Di Scala, C., Troadec, J. D., Lelièvre, C., Garmy, N., Fantini, J., and Chahinian, H. (2014) Mechanism of cholesterol-assisted oligomeric channel formation by a short Alzheimer β -amyloid peptide. *J. Neurochem.* 128, 186–195.
- (19) Mattson, M. P., Cheng, B., Davis, D., Bryant, K., Lieberburg, I., and Rydel, R. E. (1992) Beta-Amyloid peptides destabilize calcium homeostasis and render human cortical neurons vulnerable to excitotoxicity. *J. Neurosci.* 12, 376–389.
- (20) Simmons, M. A., and Schneider, C. R. (1993) Amyloid beta peptides act directly on single neurons. *Neurosci. Lett.* 150, 133–136.
- (21) Millucci, L., Ghezzi, L., Bernardini, A., and Santucci, A. (2010) Conformations and biological activities of amyloid beta peptide 25–35. *Curr. Protein Pept. Sci.* 11, 24–67.
- (22) Kubo, T., Nishimura, S., Kumagae, Y., and Kaneko, I. (2002) In vivo conversion of racemized beta-amyloid ([D-Ser 26]A beta 1–40) to truncated and toxic fragments ([D-Ser 26]A beta 25–35/40) and fragment presence in the brains of Alzheimer's patients. *J. Neurosci. Res.* 70, 474–483.
- (23) Thakur, G., Pao, C., Micic, M., Johnson, S., and Leblanc, R. M. (2011) Surface chemistry of lipid raft and amyloid A β (1–40) Langmuir monolayer. *Colloids Surf., B* 87, 369–377.
- (24) O'Neil, M. J., Ed. (2001) *The Merck Index: an encyclopedia of chemicals, drugs, and biologicals*, 13th ed., Merck, Rahway, NJ.
- (25) Fantini, J., Carlu, D., and Yahi, N. (2011) The fusogenic tilted peptide (67–78) of α -synuclein is a cholesterol binding domain. *Biochim. Biophys. Acta* 1808, 2343–23451.
- (26) Jang, H., Arce, F. T., Ramachandran, S., Capone, R., Azimova, R., Kagan, B. L., Nussinov, R., and Lal, R. (2010) Truncated beta-amyloid peptide channels provide an alternative mechanism for Alzheimer's Disease and Down syndrome. *Proc. Natl. Acad. Sci. U.S.A.* 107, 6538–6543.
- (27) Arispe, N., Pollard, H. B., and Rojas, E. (1996) Zn²⁺ interaction with Alzheimer amyloid beta protein calcium channels. *Proc. Natl. Acad. Sci. U.S.A.* 93, 1710–1715.
- (28) Vallee, B. L., and Auld, D. S. (1993) Cocatalytic zinc motifs in enzyme catalysis. *Proc. Natl. Acad. Sci. U.S.A.* 90, 2715–2718.

- (29) Simons, M., Keller, P., Dichgans, J., and Schulz, J. B. (2001) Cholesterol and Alzheimer's disease: is there a link? *Neurology* 57, 1089–1093.
- (30) Ji, S. R., Wu, Y., and Sui, S. F. (2002) Cholesterol is an important factor affecting the membrane insertion of beta-amyloid peptide (A beta 1–40), which may potentially inhibit the fibril formation. *J. Biol. Chem.* 277, 6273–6279.
- (31) Qiu, L., Lewis, A., Como, J., Vaughn, M. W., Huang, J., Somerharju, P., Virtanen, J., and Cheng, K. H. (2009) Cholesterol modulates the interaction of beta-amyloid peptide with lipid bilayers. *Biophys. J.* 96, 4299–4307.
- (32) Micelli, S., Meleleo, D., Picciarelli, V., and Gallucci, E. (2004) Effect of sterols on beta-amyloid peptide (AbetaP 1–40) channel formation and their properties in planar lipid membranes. *Biophys. J.* 86, 2231–7223.
- (33) McFarland, K., Spalding, T. A., Hubbard, D., Ma, J. N., Olsson, R., and Burstein, E. S. (2013) Low Dose Bexarotene Treatment Rescues Dopamine Neurons and Restores Behavioral Function in Models of Parkinson's Disease. *ACS Chem. Neurosci.* 4, 1430–1438.
- (34) Gandy, S., and DeKosky, S. T. (2013) Toward the treatment and prevention of Alzheimer's disease: rational strategies and recent progress. *Annu. Rev. Med.* 64, 367–383.
- (35) Brooks, B. R., Brooks, C. L., 3rd, Mackerell, A. D., Jr., Nilsson, L., Petrella, R. J., Roux, B., Won, Y., Archontis, G., Bartels, C., Boresch, S., Caflisch, A., Caves, L., Cui, Q., Dinner, A. R., Feig, M., Fischer, S., Gao, J., Hodoscek, M., Im, W., Kuczera, K., Lazaridis, T., Ma, J., Ovchinnikov, V., Paci, E., Pastor, R. W., Post, C. B., Pu, J. Z., Schaefer, M., Tidor, B., Venable, R. M., Woodcock, H. L., Wu, X., Yang, W., York, D. M., and Karplus, M. (2009) CHARMM: the biomolecular simulation program. *J. Comput. Chem.* 30, 1545–614.
- (36) Singh, R. P., Brooks, B. R., and Klauda, J. B. (2009) Binding and release of cholesterol in the Osh4 protein of yeast. *Proteins* 75, 468–477.
- (37) Thomsen, R., and Christensen, M. H. (2006) MolDock: A New Technique for High-Accuracy Molecular Docking. *J. Med. Chem.* 49, 3315–3321.
- (38) Fantini, J., and Yahi, N. (2011) Molecular basis for the glycosphingolipid-binding specificity of α -synuclein: key role of tyrosine 39 in membrane insertion. *J. Mol. Biol.* 408, 654–669.